

A Comparison of 2D-3D Intensity-Based Registration and Feature-Based Registration for Neurointerventions

Robert A. McLaughlin¹, John Hipwell²,
David J. Hawkes², J. Alison Noble¹, James V. Byrne³, and Tim Cox⁴

¹ Medical Vision Laboratory, Dept. Engineering Science, University of Oxford,
Oxford, England

`ram@robots.ox.ac.uk`

² CISG, Division of Radiological Sciences, Guy's Hospital
King's College London, London, England

`john.hipwell@kcl.ac.uk`

³ Department of Radiology, Radcliffe Infirmary, Oxford, England

⁴ National Hospital for Neurology and Neurosurgery
Queen Square, London, England

Abstract. Registration of 2D-3D data can improve visualisation during minimally-invasive neurointerventions. Using four clinical data sets, we quantitatively compared two approaches: an intensity-based algorithm and a feature-based algorithm. The intensity-based approach was found to be more accurate, with an average registration accuracy of 1.4mm, compared to the feature-based algorithm with an average accuracy of 2.3mm. The intensity-based algorithm was also found to be more reliable. Reliability of the feature-based algorithm was found to be more sensitive to the complexity of the vasculature structure.

1 Introduction

The registration of 2D-3D data sets is important in minimally invasive neuro-interventions, such as the coiling of brain aneurysms or glueing of arteriovenous malformations (AVM). During such interventions a neuro-radiologist guides a catheter through the brain vasculature using 2D X-ray images. The 2D nature of the images can make it difficult to navigate and position the catheter accurately in a complicated 3D angioarchitecture.

One solution would be to utilise a pre-operative phase contrast magnetic resonance angiography (PC-MRA) scan. Such a scan could be segmented [1][2] to produce a 3D model of the vasculature. By registering the intra-operative X-ray image with this 3D model, it would be possible to accurately display the position of the catheter relative to the 3D model.

In this paper, we compare two approaches to 2D-3D registration: an intensity-based method [3] and a feature-based method [4]. We compare accuracy and robustness of these two algorithms on four clinical data sets.

2 Method

2.1 Intensity-Based Registration

The intensity-based registration algorithm builds on the work in [3] and iteratively optimises the six rigid-body parameters describing the location and rotation of the 3D model. Digitally reconstructed radiographs (DRR) are generated by casting rays through the segmented volume, and are compared to the digital subtraction angiography (DSA) image using the gradient difference similarity measure [5]. Gradient images are computed for both the the DSA image and the DRR using 3x3 Sobel templates. The gradient difference similarity measure minimises the difference between these gradient images. Details are given in [3].

Some modifications to the algorithm of [3] were required to adapt it to work with segmented 3D data and DSA images, rather than unsegmented CT data and fluoroscopy images. The primary modification was the use of a spherical volume-of-interest (VOI), manually defined around the feature of interest (aneurysm or AVM). Only voxels lying within the VOI were used in the registration.

The VOI was projected onto the DRR as a circular mask. A concentric circular mask with one quarter the radius was then defined, and pixels within this smaller mask were used in an initial registration. The radius of the smaller mask was then doubled and this larger mask was used to refine the registration. The centre of rotation for the volume was set to be the centre of the VOI.

To reduce processing time at each stage, a multi-resolution strategy was adopted whereby the DRRs and DSA images were sub-sampled by a factor of four. These dimensions were subsequently doubled until the optimisation of the parameters was completed with both images at their full resolutions.

2.2 Feature-Based Registration

The feature-based registration algorithm [4] first skeletonises vessels in the DSA image, reducing the thickness of each to a single pixel. Blood vessels in the 3D model are also skeletonised by extracting the medial axis of each vessel. The algorithm registers the data sets by matching the skeletonised DSA image with a projection of the skeletonised 3D model. For each 3D point, the closest corresponding point in the skeletonised DSA image is found using a territory-based correspondence search as described in [4]. Using these pairs of points and the method outlined in [6], the algorithm finds the optimal rotation and translation of the 3D model to achieve a registration. The registration was performed in three stages, using the VOI defined in Section 2.1. Registration was initially performed with the small mask, refined using the larger mask and finally completed using the entire DSA image. A similar use of masks was presented in [7].

3 Experiments

3.1 Data

Phase-contrast MRA (PC-MRA) scans were obtained for three patients with aneurysms (patients 1-3) and one patient with an AVM (patient 4). Scans were

acquired on a Siemens Magnetom Vision 1.5T with voxel size $0.78 \times 0.78 \times 1.5\text{mm}$ and image dimensions $256 \times 256 \times 64$. The scans for patients 1, 2 and 4 contained flow speed information and were segmented as described in [1]. An improved scan was used for patient 3, giving both flow speed and flow direction information, and this extra information was used to give an improved segmentation [2]. Visualisations of the segmented MRA data sets are shown in Figure 1.

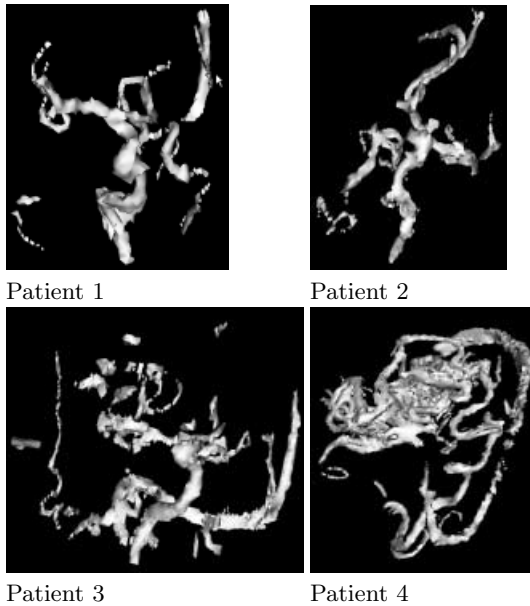


Fig. 1. 3D visualisations of segmented MRA scans.

For each patient, two DSA runs at different orientations were acquired using a GE Medical Systems Advantx DX, and digitised from the PAL composite video signal at an image resolution of 512×512 pixels using a Matrox Meteor II framegrabber. For each DSA run, three to seven images were acquired at half second intervals. These were used to generate two images: a maximal image where the images were combined so that the maximal level of contrast over the run is recorded for each pixel; and a single-frame image, where an image that had maximal opacification of the arterial system was chosen. A distortion-correction phantom and software were used to correct for pincushion distortion in the images [5]. Typical DSA images produced are shown in Figure 2.

3.2 Calculation of “Gold-Standard” Registration

Parameters for the gold-standard registration may be described as either intrinsic or extrinsic. Intrinsic parameters describe properties of the imaging system,

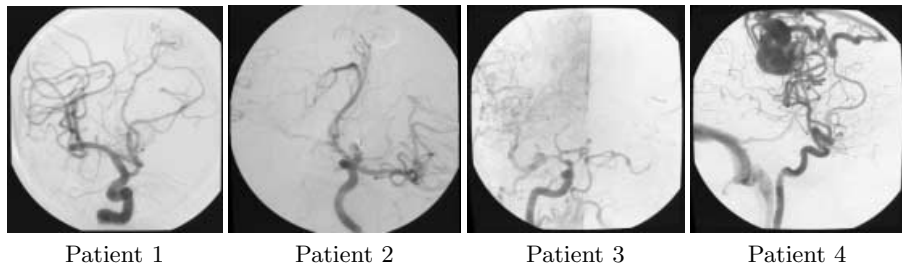


Fig. 2. The first of two DSA runs obtained for each patient. Patients 1 and 2 show single frame DSA images, while Patients 3 and 4 show maximal DSA images.

such as the perspective projection matrix. Extrinsic parameters describe the orientation (rotation) and position (translation) of the 3D model [5]

Intrinsic parameters for the gold standard registration were computed from parameters obtained from the X-ray machine display during acquisition. As no fiducial markers were available in either the PC-MRA scans or the DSA images, the extrinsic parameters were obtained by a manual registration performed by JVB (neuro-radiologist). The manual registration was performed using 3D visualisation software which simulated X-ray images for a specified translation and rotation, allowing the neuro-radiologist to align clinically relevant points in the images. To test the stability of these manual results, registrations for patient 2: DSA run 1 and patient 4: DSA run 1 were each repeated eight times, and variation in the results were computed using the reprojection distance described in the next section.

3.3 Experiments for Accuracy and Robustness

The segmented MRA data sets were registered with both maximal and single-frame DSA images. Starting positions for the registrations were chosen by perturbing the gold standard values by set amounts. This methodology was used in [5]. Four experiments were performed, with the amount of perturbation increased each time, as shown in Table 1. For each experiment, different combinations of the four perturbations resulted in sixteen different starting positions. Note that there were no in-plane translations (δX or δY), as these can be accurately calculated by selecting a single corresponding point in both the DSA image and the DRR simulated from the MRA data.

To measure accuracy, the reprojection distance was used, as defined by Matsutani et al. [8]. A number of anatomically visible points on the segmented 3D model were chosen, along with the corresponding points in the DSA image. Using the rotation and translation matrix resulting from each registration, the position of the 3D points was recomputed. The minimum distance (in mm) from each point to the ray passing from the X-ray source to the corresponding DSA image point was then calculated. This gave a measurement of the accuracy of the registration when projecting from 3D to 2D. A discussion of the measurement

Table 1. Perturbations of the starting positions from the gold standard for four of the six rigid-body parameters.

Experiment #	δZ	$\delta\theta_x$	$\delta\theta_y$	$\delta\theta_z$
1	± 25 mm	$\pm 4^\circ$	$\pm 4^\circ$	$\pm 4^\circ$
2	± 50 mm	$\pm 8^\circ$	$\pm 8^\circ$	$\pm 8^\circ$
3	± 75 mm	$\pm 12^\circ$	$\pm 12^\circ$	$\pm 12^\circ$
4	± 100 mm	$\pm 16^\circ$	$\pm 16^\circ$	$\pm 16^\circ$

can be found in [5]. Finally, the average RMS error of all such points for each experiment was computed. If the average RMS error for a particular registration was less than 4 mm, the registration was judged to have succeeded.

4 Experiment and Results

Figure 3a plots registration accuracy for each algorithm, using both the maximal DSA images and the single-frame DSA images. These are plotted against the variability in the manual 'gold-standard' registration, which was computed as 1.7mm. Figure 3b plots the percentage of successful registrations. Only successful registrations were used in computing the accuracies shown in figure 3a. Results of typical registrations are displayed in figure 4.

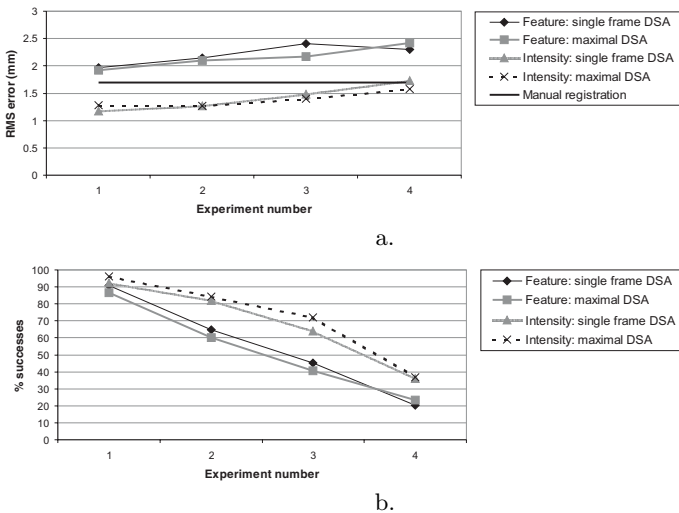


Fig. 3. (a) Registration accuracy. (b) Registration reliability.

The percentage of successful registrations varied with the data sets, being notably higher with Patients 1 and 2 than with Patients 3 and 4. Graphs showing the percentage of successful registrations with each data set are shown in figure 5.

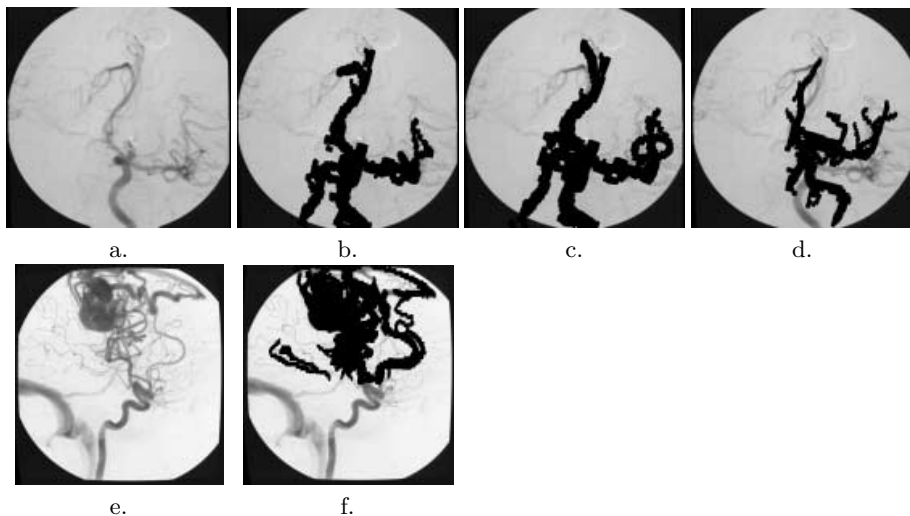


Fig. 4. Results of registration. Registered 3D vessels are overlaid in black. (a) Original DSA image for Patient 2. (b) Typical successful registration for patient 2. (c, d) Failed registrations for patient 4. (e) Original DSA image for Patient 4. (f) Typical successful registration for patient 4.

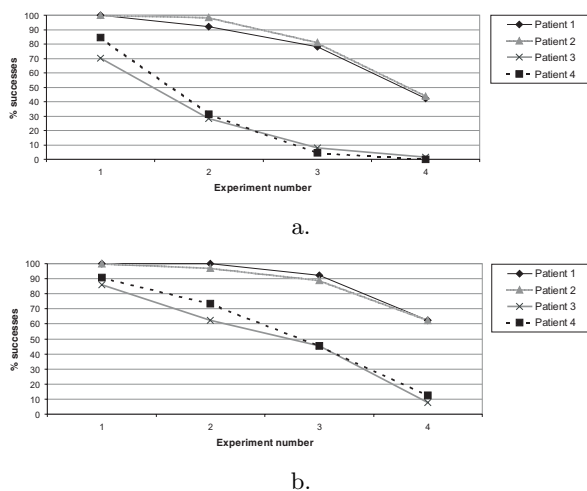


Fig. 5. Registration reliability for each patient data set. (a) Feature-based algorithm. (b) Intensity-based algorithm.

5 Discussion

The intensity-based algorithm had the greater accuracy of the two algorithms, with an average accuracy of 1.4mm. This compared to an average value of 2.3mm

for the feature-based algorithm. Recall that the feature-based algorithm registers a skeleton of the 3D model with a skeleton of the DSA image. It is thus sensitive to inaccuracies in the position of the 2D and 3D skeletonised points. This accounts for its lower accuracy when compared to the intensity-based algorithm, which registers the intensity values of every individual pixel. Note that the difference in image quality between the maximal and single-frame DSA images did not noticeably alter the accuracies for either algorithm.

The intensity-based algorithm was also more robust. This is in contrast to the experimental results of [7], which found the feature-based algorithm to be more robust. The experiments in [7] were performed using the far simpler vasculature of an in-vitro silicon aneurysm phantom (middle cerebral artery bifurcation aneurysm). Our results suggest that while for simple angioarchitectures the feature-based approach may be more robust, in complicated situations the intensity-based approach is superior. The results in figure 5 support this conclusion. The robustness trends shown in the graphs fall into two distinct classes, with Patients 1 and 2 proving to be more robust than Patients 3 and 4. Recall that while the scans for Patients 1 and 2 contained only flow speed information, Patient 3 contained both flow speed and direction information. This led to a more complicated segmentation, with small vessels detected. Patient 4 was complex due to the angioarchitecture of the AVM. These results suggest that robustness of the feature-based approach could be greatly improved if, in some initial stage of processing, the vasculature in the 3D model and DSA image could be simplified to contain only the most significant vessels.

An essential difference between the two algorithms lies in the method by which they combine conflicting information and iteratively improve the current state of the registration. The intensity-based algorithm tests each minor perturbation to the current rotation and translation, minimising a similarity measure that is summed over the entire data set. In contrast, in the feature-based algorithm each pair of matching points (one from the 3D skeleton and one from the skeletonised DSA image) specify an optimal change to the present rotation and translation. It is the average rotation and translation that is chosen. This method renders the algorithm sensitive to a misregistration of one or two erroneous vessels, as these will produce greatly different estimates for the rotation and translation. This suggests that the use of a robust fitting method such as RANSAC [9] may greatly improve the reliability of the feature-based algorithm.

The computation time of the algorithms has important ramifications for the clinical suitability of either approach to registration. The feature-based algorithm is far less computationally intensive than the intensity-based algorithm, resulting in a much faster registration. This is because the feature-based algorithm operates on a small number of skeletonised points, rather than the exhaustive pixel-based approach of the intensity-based algorithm. In future work, we will seek to quantify these differences.

6 Conclusion

We have compared an intensity-based and a feature-based registration algorithm for the registration of 3D PC-MRA data to DSA images. The algorithms were tested using four clinical PC-MRA data sets and eight DSA runs. The intensity-based registration algorithm produced more accurate registrations, with an average RMS reprojection error of 1.4 mm. The feature-based algorithm was found to have an average RMS reprojection error of 2.3 mm.

The intensity-based algorithm was found to converge to the correct solution with greater reliability. Our results suggest that reliability of the feature-based algorithm are more effected by the complexity of the angioarchitecture than is the intensity-based method. In future work we will explore whether the feature-based approach may be made more reliable by the incorporation of a robust fitting method.

Acknowledgements

We wish to thank Dr. G. P. Penney, K. Rhode, Dr. A.C.S. Chung and Dr. Y. Kita for their help in undertaking this research. This work was supported by ESPRC grants GR/M55008 and GR/M55015.

References

1. Chung, A.C.S., Noble, J.A.: Statistical 3D vessel segmentation using a Rician distribution. In: Proc. MICCAI. (1999) 82–89
2. Chung, A., Noble, J.: Fusing magnitude and phase information for vascular segmentation in phase contrast mr angiograms. In: Proc. MICCAI. (2000) 166–175
3. Penney, G.P., Weese, J., Little, J.A., Desmedt, P., Hill, D.L.G., Hawkes, D.J.: A comparison of similarity measures for use in 2d-3d medical image registration. *IEEE Transactions on Medical Imaging* **17** (1998) 586–595
4. Kita, Y., Wilson, D.L., Noble, J.A.: Real-time registration of 3D cerebral vessels to X-ray angiograms. In: MICCAI'98. (1998) 1125–1133
5. Penney, G.P.: Registration of Tomographic Images to X-ray Projections for Use in Image Guided Interventions. Phd thesis, University College London, CISG, Division of Radiological Sciences, Guy's Hospital, King's College London, London SE1 9RT England (2000)
6. Heuring, J.J., Murray, D.W.: Visual head tracking and slaving for visual telepresence. In: Proc. of IEEE Int. Conf. on Robotics and Automation. (1996) 2908–2914
7. McLaughlin, R.A., Hipwell, J., Penney, G.P., Rhode, K., Chung, A., Noble, J.A., Hawkes, D.J.: Intensity-based registration versus feature-based registration for neurointerventions. In: Proceedings of Medical Image Understanding and Analysis (MIUA). (2001) 69–72
8. Masutani, Y., Dohi, T., et al., F.Y.: Interactive virtualized display system for intravascular neurosurgery. In: CVRMed-MRCAS'97. (1997) 427–435
9. Fischler, M.A., Bolles, R.C.: Random sample consensus: A paradigm for model fitting with applications to image analysis and automated cartography. *Communications of the ACM* **24** (1981) 381–395